International Journal of Science and Research Archive
eISSN: 2582-8185
Cross Ref DOI: 10.30574/ijsra
Journal homepage: https://ijsra.net/

(RESEARCH ARTICLE)

Check for updates

Investigation on stress-seepage variation characteristics around coal mine goaf

Tao Liu * and JiaTong Li

School of Safety Science and Engineering, Anhui University of Science and Technology, Huainan 232001, China.

International Journal of Science and Research Archive, 2026, 18(02), 530-541

Publication history: Received on 04 January 2026; revised on 09 February 2026; accepted on 11 February 2026

Article DOI: https://doi.org/10.30574/ijsra.2026.18.2.0262

Abstract

To investigate stress-seepage change characteristics around goaf area, a theoretical damage-based model on gas flow was established. Distribution characteristics of stress and fractures during coal mining and damage-based gas flow properties were analyzed. Results reveal that coal mining leads to a symmetrical distribution of stress field about the middle of working face, while stress concentration occurs at both ends of goaf. As the mining working face advances, stress concentration degree at both ends increases. Meanwhile, stress-relief range above and below working face increases significantly, with a better stress-relief effect observed within 30m from goaf floor. Stress release rate is mostly above 85%. As coal mining progresses, plastic damage surrounding goaf area also expands and intensifies, resulting in formation of a plastic damage zone with a 'saddle' shape once the working face advances to 160 meters. Due to significant impact of damage, coal permeability within 10 meters from the floor of goaf increases sharply. Permeability near the floor of goaf could rise by about 830 times, leading to a substantial rising in gas emission rate in stress-relief floor layer. These results could provide effective theoretical reference for preventing and controlling gas-related incidents around goaf.

Keywords: Gas Control; Permeability Sharp Increase; Stress Field; Coal Mine Goaf

1. Introduction

Most of coal mining activities around world have been going deeper and deeper. However, deep coal seams are accompanied by high ground stress, high gas and low permeability, which easily lead to coal and gas outburst accidents and threaten the safe production of coal mines. Furthermore, these accidents could cause major injuries, deaths and economic property losses, seriously affecting efficient and safe coal production[1,3]. At present, several outburst prevention methods have been proposed, including regional comprehensive outburst control methods and local comprehensive outburst control methods. Among different regional outburst control methods, mining the protective layer to realize stress relief and permeability improvement is one of the effective ways[4]. It has a significant outburst prevention effect when combined with pressure-relief gas extraction methods[5, 6]. Therefore, it is of great theoretical and practical significance to establish a theoretical model of multi-physical field coupling in coal seams to study stress, damage and gas flow characteristics around coal mine goaf in the process of protective coal seam mining.

Regarding the changes in stress and permeability characteristics of coal induced by protective seam mining, scholars have conducted some studies and achieved many meaningful results. In terms of stress changes, Zhang et al.[7] analyzed permeability change patterns of three types of coals (intact, ruptured, and broken) under different stress paths. By carrying out similar simulation tests for coal seam mining, Ren et al.[8] analyzed the stress variation laws of the protective and protected seams. Through indoor tests, Kang et al.[9] concluded that the multiplication of the horizontal stress increase can be used as a reference value for the degree of roof collapse in the coal mine goaf. Wang et al.[10] found that a larger bearing in the targeted mine goaf led to a lower loading on the solid surrounding rock, and vice versa. Xie et al.[11] analyzed the stress evolution law under three coal mining methods. The results showed similar patterns

* Corresponding author: Tao Liu

of coal mechanical properties under three mining methods, and the mechanical parameters during coal destruction can be linearly characterized. In terms of fissures, Zhang et al.[12] quantitatively analyzed the scale distribution characteristics of micropore fissures and the spatial distribution of the mining fissure network of coal-rock under three typical mining methods. By performing similarity tests on multiple coal seams, Zhang et al.[13] obtained the fracture variation law of overlying strata affected by repeated mining conditions combined with field measurement data. Li et al. [14] analyzed the evolution of overburden fissures under single-seam mining and overlay mining conditions. Impacting principle of the overlay mining on fissures in overlying strata was revealed. Zhao et al.[15] obtained the fissure evolution law of overlying rocks in big mining height cases in composite roofs. Zhang et al.[16] analyzed the effect of small burial depth on fissure and permeability properties. In terms of gas flow, Pan et al.[17] reviewed the permeability of coal and its behavioral modeling methods, concluding that coal permeability decreases exponentially with increasing effective stress. Wang et al.[18] concluded that the permeability of water-resisting layer increases by about two to three orders of magnitude from the initial permeability as the advance distance of the stope face increases. Zhang et al.[19] conducted cyclic seepage loading-unloading tests on crushed coal. They found that stress sensitivity of permeability of crushed coal samples during unloading was negatively correlated with the secant modulus. Wang et al.[20] analyzed the specific influences of factors such as the Klinkenberg effect and matrix gas diffusion on coal seam gas transport.

It could be seen that previous studies have mainly focused on changes in stress and fracture properties variations induced by first mining of protective layer. Damage to coal around mining goaf and its enhancement mechanism on coal permeability and gas seepage needs further investigation. Therefore, this study analyzes mechanical damage characteristics around the goaf based on COMSOL Multiphysics software, as well as gas flow pattern in stress-relief coal seam experiencing damage effect. Results could provide theoretical basis for gas control and safe mining of deep coal seams.

2. Theoretical model

Stress-strain curve of rocks could be categorized as four stages. Resulted from external force, coal sample enters the first stage (i.e., the compaction stage), during which, cracks and holes inside coal are gradually closed under pressure. As stress rises, coal enters second stage (i.e., elastic deformation stage). Fractures inside coal is in state of compression closure. Stress-strain curve begins to exhibit linear variations. After stress reaches yield point, coal sample enters third phase (i.e., plastic deformation phase). New cracks appear inside the coal sample and continuously expand. Many microcracks sprout, gradually becoming a microcrack zone. The fourth stage (i.e., the failure stage) starts after the peak stress is reached. In this stage, a sharp decrease appears on stress-strain curve. Internal pore-crack structure of coal dramatically expands, and macrocracks on the surface are penetrated, leading to damage of coal sample. When the stress reaches the post-failure stage, tensile and shear damage occurs in coal under different stress scenarios[21-25]. Tensile damage begins while coal stress satisfies first strength theory (i.e., C_1). Shear damage occurs when the Moore-Coulomb criterion is satisfied (i.e., C_2). These two criteria could be expressed as[26]:

$$\begin{cases} C_1 = \sigma_1 - f_{t0} = 0 \\ C_2 = \sigma_1 \left[\frac{1+sin\,\emptyset}{1-sin\,\emptyset}\right] - \sigma_3 - f_{c0} = 0 \end{cases} \quad (1)$$

where σ_1 represents maximum principal stress, MPa; σ_3 denotes minimum principal stress, MPa; f_{t0} represents uniaxial tensile strength, MPa; f_{c0} denotes uniaxial compressive strength, MPa; ∅ denotes internal friction angle, °.

In the state of uniaxial tensile stress, mesoscopic damage constitutive model could be expressed by Equation (2)[27]:

$$G = \begin{cases} \text{Non damage } (\mathrm{M} \le \mathrm{M_{t0}}) \\ 1 - \frac{F_{tr}}{ME_0} \quad (M_{t0} < M \le M_{tu}) \\ \text{Damage } (M > M_{tu}) \end{cases} \quad (2)$$

where G is damage variable, G=0 corresponds to no damage, 0<G<1 means damage in different levels, G=1 corresponds to complete damage; M_{t0} represents tensile strain at elastic limit; M denotes tensile strain; F_{tr} denotes residual strength of the unit, MPa; E_0 denotes initial modulus of elasticity, MPa; M_{tu} represents tensile strain in ultimate state.

Under uniaxial compressive stress, mesoscopic damage constitutive relationship could be expressed by Equation (3)[27]:

$$G = \begin{cases} 0 & (M \le M_{c0}) \\ 1 - \frac{\gamma M_{c0}}{M} & (M > M_{C0}) \end{cases} \qquad (3)$$

where γ is unit residual strength coefficient; M_{C0} represents maximum compressive principal strain.

Based on cubic law of pore-permeability of coal, impact of coal damage to permeability is considered, permeability change relationship could be expressed as follows[26]

$$\frac{k}{k_0} = \left(\frac{\phi}{\phi_0}\right)^3 \exp(\alpha_k G) \qquad (4)$$

where ϕ_0 is initial porosity; k_0 is initial permeability coefficient, m2; α_k is the damage coefficient; G is the damage variable.

Based on Darcy's law and flow continuity equation, partial differential equation of seepage is:

$$\frac{\partial}{\partial t}(\phi\rho) + \nabla\rho\left(-\frac{k}{u}\nabla p\right) = Q_{\mathrm{m}} \qquad (5)$$

where ρ represents gas density, kg/m3; ϕ denotes porosity; k is permeability, m2; u represents fluid viscosity, Pa·s; Q_m is source-sink term, Kg/m3·s; p denotes pressure, Pa.

3. Establishment of numerical model

The Ji15 and Ji16-17 coal seams of target mine are the main coal seams. Meanwhile, Ji16-17 seam is below Ji15 seam. There is a mudstone layer between them. Thickness of mudstone is 3.4m. In order to analyze the influence of initial overlying coal seam mining on lower coal beds, COMSOL Multiphysics software was used to simulate Ji15 seam mining process. Due to proximity of these two seams, gas from Ji16-17 seam will be discharged to Ji15 mining working face and goaf area during initial mining of Ji15 seam, increasing possibility of gas accident.

Based on the above situation, stress relief and gas extraction need to be conducted in advance. The model uses Ji15 coal seam as first-mining coal seam and Ji16-17 coal seam as stress-relief layer. Length of the model is 300 m, and the height is 247 m, of which the length of the first-mining protective layer is 160 m and the height is 3.6 m. In-situ stress of Ji15 coal seam is about 18 MPa. Loading is applied at model's top boundary. Fixed constraints are applied at the bottom and two side boundaries of the model. Because a denser model mesh results in more accurate calculations, the mesh is set more densely in the area near the first mining layer of the working face. The numerical model is illustrated in Figure 1. Coal mechanical parameters within model range are shown in Table 1.

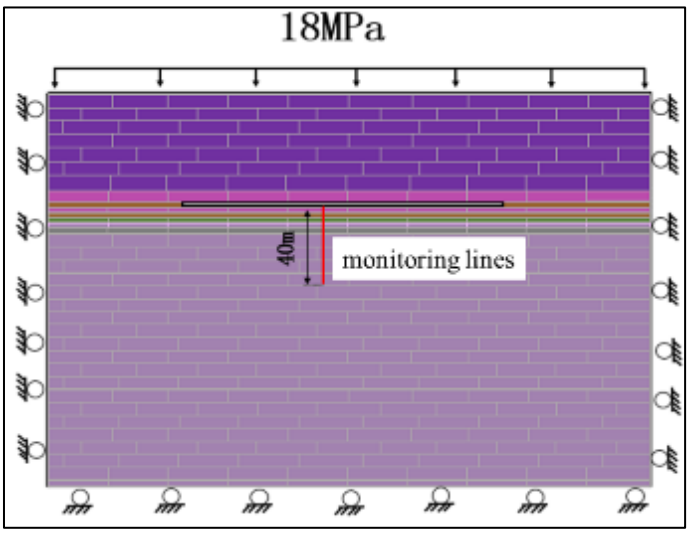

Figure 1 Numerical simulation model

Table 1 Coal rock mechanics parameters

Rock name	Model color	Layer thickness/m	Density/(kg • m^{-3})	Young's modulus /GPa	Poisson's ratio	Friction angle / (°)	UTS /MPa	UCS /MPa
Medium-grained sandstone		60	2100	8	0.31	29	0.96	39
Mudstone		6	1500	2.2	0.35	25	0.67	23
Ji15 coal		3.6	1250	1.3	0.39	20	0.50	16
Mudstone		3.4	1500	2.2	0.35	25	0.67	23
Ji16-17 coal		1.8	1280	1.5	0.38	21	0.58	18
Sandy mudstone		4	1720	3.9	0.32	26	0.85	30
Fine sandstone		2.4	2300	16	0.3	31	1.03	50
Limestone		5.5	2650	24	0.29	35	1.16	63
Fine sandstone		160	2300	16	0.3	31	1.03	50

4. Result analysis and discussion

4.1. Stress variation

4.1.1. Stress field distribution characteristics

Before mining activities, coal is in hydrostatic pressure condition. Stress is uniformly distributed on coal. Vertical stress at each point is the original stress. Coal mining disturbed the equilibrium of stress field in the original rock and redistributed the stresses[28]. Due to different intensities of the bearing stresses between coal pillar and coal mine goaf, the overlying loads were transferred and redistributed. Part of the overburden load was carried by coal wall at two ends of mining goaf. Consequently, stress of coal wall at both ends of mining area is significantly increased, forming a high-stress concentration area[29-31]. Figure 2 shows cloud map of vertical stress distribution around mining area for different mining advancement distances of first-mining layer. It can be seen that stress is reduced in the upper and lower areas of coalmine goaf. Stress-relief zone is similar to an ellipse, and a stress concentration can be clearly observed at two ends of working face in mining goaf. With coal mining advancement, advancing length increases, and peak stress becomes larger, with a more apparent stress concentration near ends of working face and an expanding effect range.

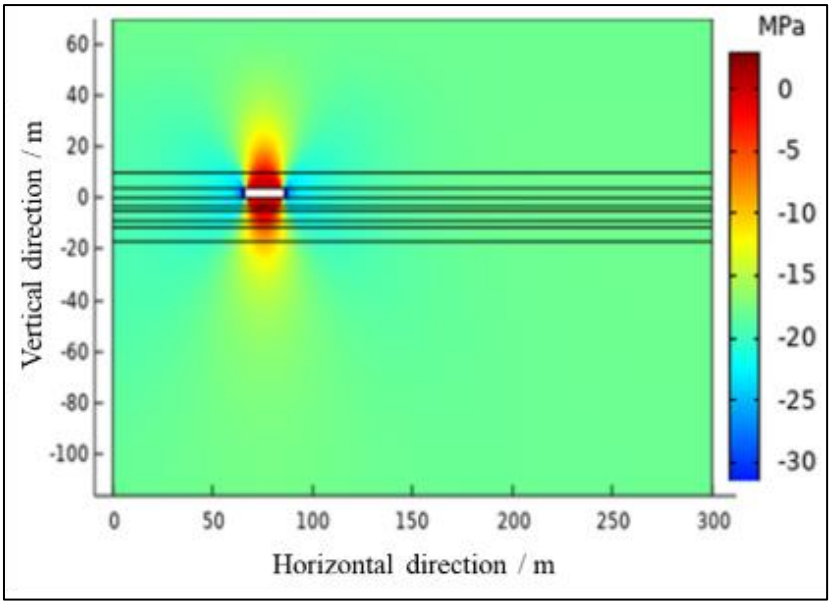

Mining length L=20m

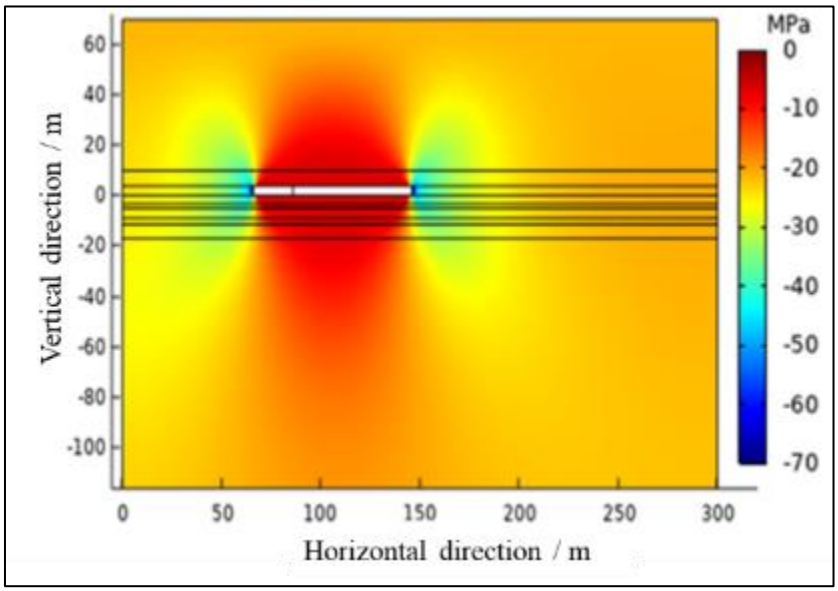

Mining length L=80m

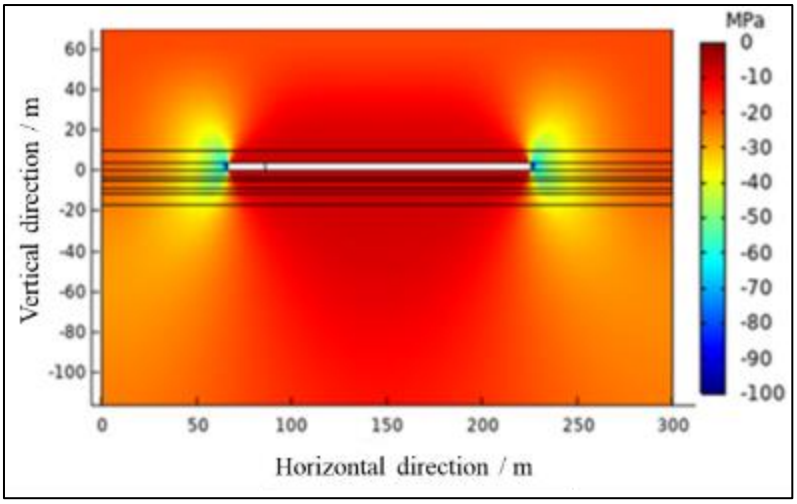

Mining length L=160m

Figure 2 Stress change characteristics during coal mining

Figure 3 is an elevation map of stress variation as the mining face advances 160 m. Depression area in the middle of mining working face represents stress reduction in that area. With the increase of advancing distance, stress on the bottom surface of coal mine goaf is gradually released, resulting in a localized transformation from compressive stress to tensile stress. The ultimate compressive threshold of coal below working face is higher than ultimate tensile threshold, and the original condition of coal is broken, leading to bending and deformation that expands to mining area. Raised ends of mining working face indicate a stress concentration in this area, with a higher degree of stress concentration in the area closer to two ends of working face.

Figure 4 reflects vertical stress variations at several advancement length of mining working face. As mining progresses, stresses in the original stress concentration areas are released, and the area of influence is gradually increasing. The peak stress increases and finally stabilizes. Compared to the stress at 20 m advancement distance, the peak stresses at 80 m and 160 m advancement distances are about 2 and 3.5 times higher, respectively. On both sides of mining goaf, coal undergoes stages of stress-concentrated compression, stress-relief expansion and post-mining stress-compression stabilization.

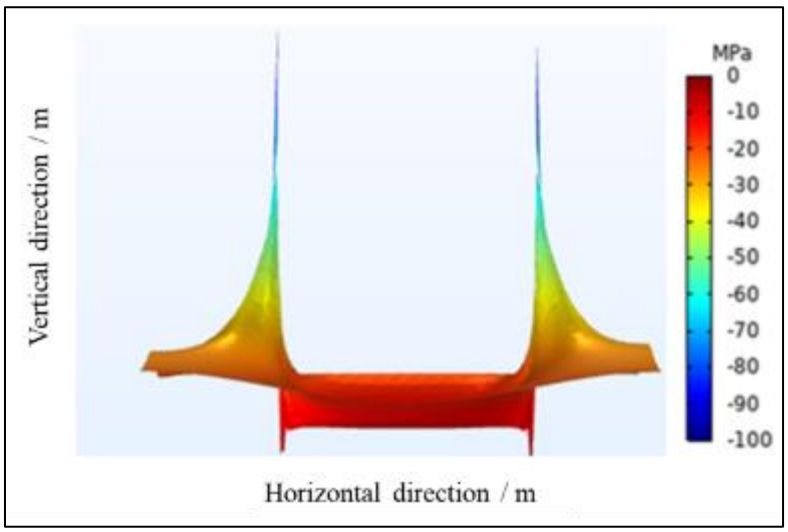

Figure 3 Elevation map of stress change when mining working face advances 160 m

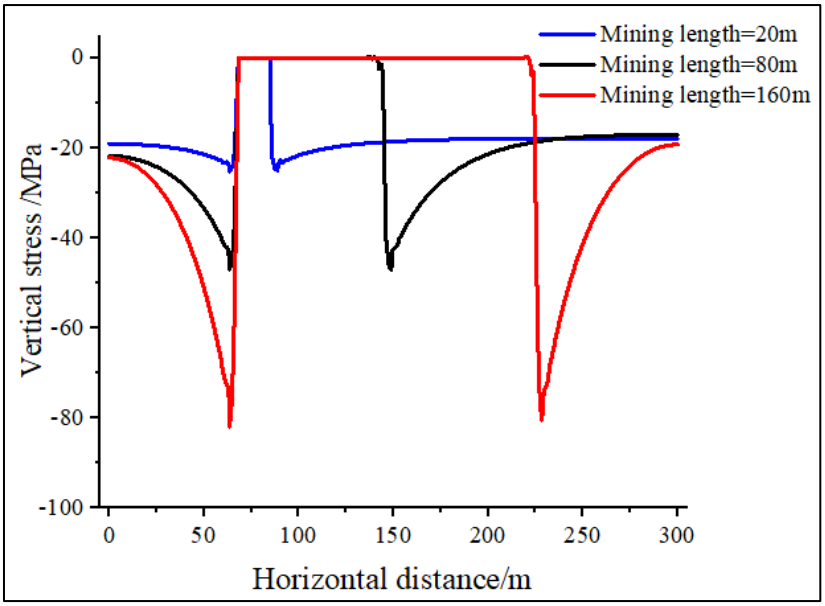

Figure 4 Variation of stress peak around goaf corresponding to different mining lengths

4.2. Stress relief analysis

First mining of upper Ji15 coal seam redistributes stress field in Ji16-17 coal seam below, releasing stresses in certain areas with varying degrees. In order to ensure that stress-relief layer is located within adequate stress-relief area caused by first-mining layer, determining stress-relief range is needed. When coal seam expansion rate increases by 0.2%-0.3%, coal seems full stress relief could be achieved. The 0.3% expansion rate could be regarded as critical value for full stress relief and permeability improvement. For burial depths of about 800 m, coal seems expansion rate is more than 0.3% only when the stress-relief ratio is 0.159[32, 33]. Since the original stress of model is 18 MPa, stress value should drop below 2.862 MPa when reaching full stress relief.

Range of vertical stress relief under mining area corresponding to different mining lengths is shown in Table 2. It could be seen that effect of stress concentration at boundary of Ji16-17 coal seam gradually increases with advancement of coal mining face. In addition, the range of full stress-relief area in Ji16-17 coal seam also rises, and proportion of full stress-relief area increases from 3.8% to 15.17% when the advance distance being from 20 m to 56 m. Throughout the mining process, the difference between the full stress-relief range of Ji16-17 seam and the advancement distance of coal mining face always maintains at about 10 m.

Table 2 Stress relief properties of lower Ji16-17 coal seam under different mining lengths

Mining length/m	Maximum vertical stress/MPa	Fully stress-relief zong/m	Fully stress-relief ratio/%
20	22.51	11.4	3.8
56	32.41	45.51	15.17
70	36.67	59.32	19.77
80	40.07	69.7	23.23
98	45.98	86.89	28.96
112	50.88	100.38	33.46
160	67.02	149.1	49.7

In order to quantitatively analyze stress-relief characteristics, concept of relief rate is defined by Equation (6). When stress-relief rate is 0, stress at that point is original stress, with no changes in stress magnitude. When stress-relief rate is less than 0, there is a stress concentration at this point rather than a stress reduction (compressive stress in the simulation is negative). When stress-relief rate is greater than 0, there is a reduction in stress at that point, with a 100% stress-relief rate indicating full stress relief at that point. When stress-relief rate is greater than 100%, stress at that

point has changed from compressive stress to tensile stress. At this time, coal seam is subjected to tensile stress and undergoes expansion and deformation. A large number of layerwise and vertical fissures are produced, increasing permeability of coal.

$$Y = \frac{\lambda_1 - \lambda_2}{\lambda_1} \tag{6}$$

where Y represents decompression rate; λ_1 is original stress; λ_2 is stress at that point.

Distribution of stress-relief rates of coal rocks at different distances under mining goaf is shown in Figure 5. It shows that stress-relief effect of coal seams 10 m away from goaf is very significant (excluding the stress concentration part at two ends). The stress-relief rate is above 95%. In coal rock seams 10-30 m away from mine goaf, stress-relief effect is also good, with most of stress-relief rate above 85%. In coal-rock seams 30-50 m away from goaf area, stress-relief effect gradually decreases, and only a small part of area could achieve full stress relief. When the distance is above 50 m, stress-relief effect is not good due to other factors including long distance to goaf.

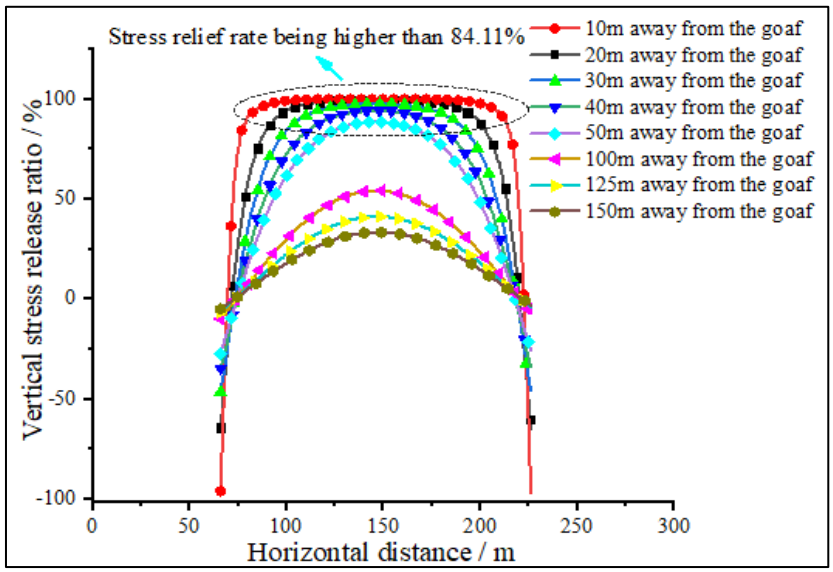

Figure 5 Vertical stress diagram of rock strata at different distances below goaf floor

4.3. Damage-based seepage characteristics in coal

In the boundary influencing zone of mining area, rock formation is not subjected to synchronized subsidence and deformation because of different supporting capacities of coal pillar and coal mine goaf for overlaying strata. Mining fissures are highly developed and difficult to compact and close, forming a fissure development zone around mining area that is "O-shaped" in cross-section and "saddle-shaped" in longitudinal section. Fissure development degree is one of the key aspects influencing permeability[34, 35].

Rupture of rock strata is a gradual process. Change of plastic damage zones around goaf under different advance distances is shown in Figure 6. When the advancing distance is 20 m, shear stress generated at two ends of the mine goaf does not reach the limit of rock damage strength. Surrounding rock of mine goaf is only elastically deformed without the formation of plastic damage zone (Figure 6a). With increasing advancing distance, range of plastic zone increases. Meanwhile, compression and shear stress intensifies, exceeding the limit of rock damage strength. It could be seen that an irregular outwardly expanding plastic damage zone is slowly formed around coal mine goaf. As the advancing distance reaching 80 m, yield damage zone appears on both sides of roof and bottom surface in coal mine goaf. Moreover, the scope of damage zone gradually increases and extends to both ends with continuous mining. When the advancing distance is 160 m, a "saddle-shaped" fissure development area is formed on the roof and bottom surface of coal mine goaf.

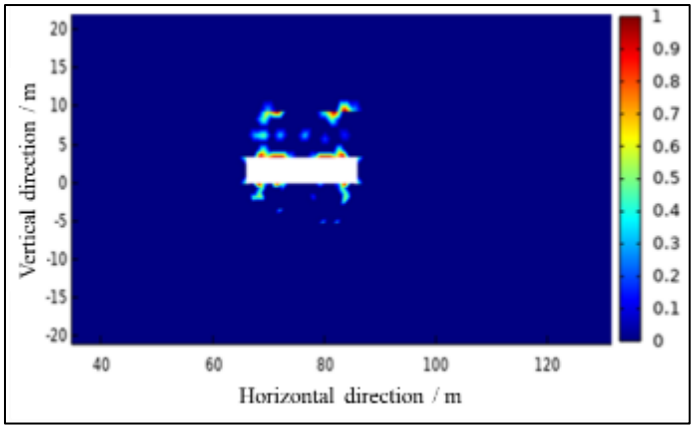

Mining length L=20m

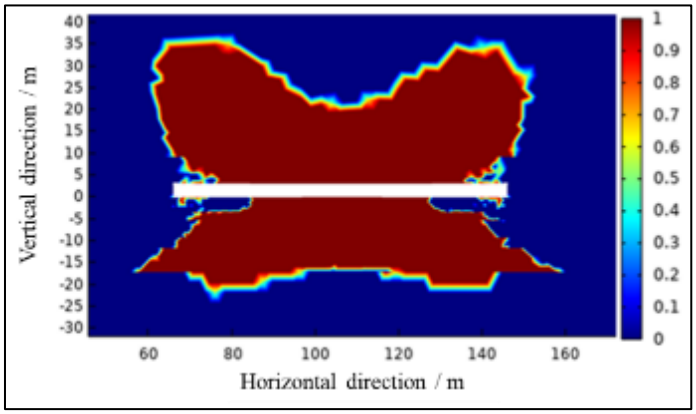

Mining length L=80m

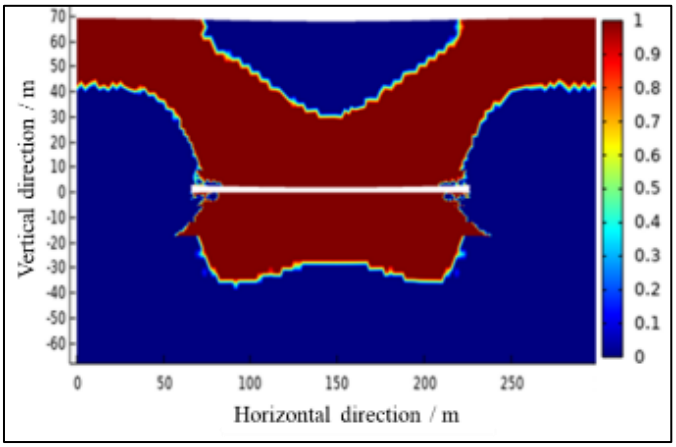

Mining length L=160m

Figure 6 Variations of plastic failure zone around goaf

Under the consideration of coal damage, numerical modeling was used to analyze changes of permeability underneath coal mine goaf. Results are shown in Figure 7. Permeability value close to goaf area increases by a approximately 830 times due to coal damage effect. Afterward, the increasing rate of permeability decreases with increasing distance from coal mine goaf. When this distance is greater than 10 m, the degree of damage to coal decreases, and increase in permeability is significantly reduced and gradually stabilized.

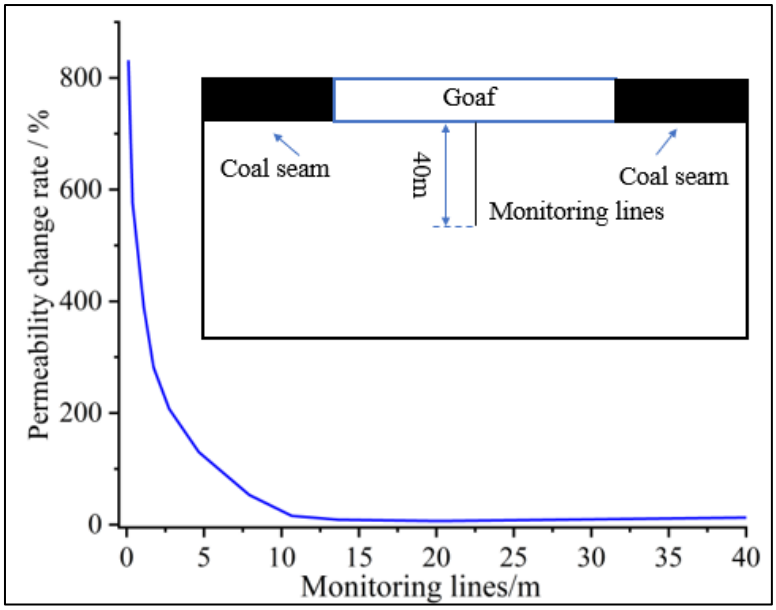

Figure 7 Permeability changes under goaf area

Under the influence of changing permeability, gas pressure below mining goaf is positively correlated to distance from goaf area and negatively correlated to the duration of gas emission. In the first 100 hours, reduction in gas pressure below goaf is insignificant. Afterward, the pressure decreasing rate gradually increases with increasing gas emission time. After approximately 300 hours of gas emission, gas pressure is below original pressure value throughout entire 5 m monitoring area below coal mine goaf. After 300 hours, 500 hours, 700 hours, 900 hours and 1100 hours of emission, gas pressure in stress-relief coal seam drops to 1.16 MPa, 1.09 MPa, 1.02 MPa, 0.95 MPa and 0.87 MPa on average, respectively.

5. Conclusion

Affected by coal mining activities, stress concentration occurs at both ends of the coal mine goaf. Meanwhile, degree of stress concentration is positively correlated to advancing distance of mining working face. An irregular stress-relief area is formed above and below working face of mining goaf. Fully stress-relief range of rock strata below goaf area is larger than that above it. Furthermore, shape of stress-relief area changes from semi-circular to semi-elliptical. Within 30 m from working face, stress relief of rock strata is almost greater than 85%. When the distance exceeds 30 m, stress-relief rate gradually decreases. Range of full stress relief becomes smaller.

Plastic damage zones appear around coal mine goaf combinedly impacted by mining disturbance and stress variation. With rising mining length, damaged zone continues to develop (the scope is expanding, as well as the degree being increasing). While working face advances to 160 m, a "saddle-shaped" plastic damage zone is formed.

Under the influence of coal damage and stress reduction, permeability within 10 m from bottom surface of goaf area significantly rises. Permeability value in the area near mining goaf could increase by a factor of approximately 830. This substantially increases velocity of gas emission from stress-relief layer below mining area, for which, specific gas control measures should be adopted for clean gas extraction.

Compliance with ethical standards

Acknowledgments

This work is financially supported by Unveiled list of bidding projects of Shanxi Province (No. 20201101001).

Disclosure of conflict of interest

No conflict of interest to be disclosed.

References

[1] Xie H, Wang J, Wang G, Ren H. New ideas of coal revolution and layout of coal science and technology development. Journal of China Coal Society. 2018;43(05):1187-97.

[2] Li S, You M, Li D, Liu J. Identifying coal mine safety production risk factors by employing text mining and Bayesian network techniques. Process Safety and Environmental Protection. 2022;162:1067-81.

[3] Zou Q, Zhang T, Cheng Z, Jiang Z, Tian S. A method for selection rationality evaluation of the first-mining seam in multi-seam mining. Geomechanics and Geophysics for Geo-Energy and Geo-Resources. 2022;8(1):17.

[4] Jiang N, Lv K, Gao Z, Di H, Ma J, Pan T. Study on Characteristics of Overburden Strata Structure above Abandoned Gob of Shallow Seams-A Case Study. Energies. 2022;15(24):9359.

[5] Huang X, Wang K, Sun D. Study on Penetration Drainage Bore-hole Reasonable Layouts in Bottom Roadway of Protected Coal Seam. World Sci-Tech R & Dq. 2011;33(04):608-10.

[6] Luo S, Wang T, Wu Y, Xie P, Shi H. Experiment on Space-Time Evolution Characteristics of Deformation and Failure of Overlying strata in Longwall Mining of Steeply Dipping Coal Seam. Energy Exploration & Exploitation. 2023;41(2):656-76.

[7] Zhang L, Kan Z, Zhang C, Tang J. Experimental study of coal flow characteristics under mining disturbance in China. International Journal of Coal Science & Technology. 2022;9(01):1-16.

[8] Ren W, Zhou H, Xue D, Wang L, Rong T, Liu J. Mechanical behavior and permeability of coal and rock under strong mining disturbance in protected coal seam mining. Journal of China Coal Society. 2019;44(01):1473-81.

[9] Kang H, Lou J, Gao F, Yang J, Li J. A physical and numerical investigation of sudden massive roof collapse during longwall coal retreat mining. International Journal of Coal Geology. 2018;188(01):25-36.

[10] Wang P, Feng G, Zhao J, Yoginder P C, Wang Z. Effect of longwall gob on distribution of mining-induced stress. Chinese Journal of Geotechnical Engineering. 2018;40(07):1237-46.

[11] Xie H, Zhou H, Liu J, Gao F. Mining induced mechanical behavior in coal seams under different mining layouts. Journal of China Coal Society. 2011;36(07):1067-74.

[12] Zhang Z, Zhang R, Xie H, Gao M, Xie J. Mining-induced coal permeability change under different mining layouts. Rock Mechanics and Rock Engineering. 2016;49(09):3753-68.

[13] Zhang J, Zhang J, Liu Q, Zhou F. Crack development and alr leakage law of overburden rock in shallow fully mechanized face. Coal Engineering. 2021;53(03):118-23.

[14] Li J, Wang S, He Y, Wang L, Zhao M. Fissure evolution of goboverlying strata under superimposed mining in coal seams group. Coal Engineering. 2021;53(12):92-6.

[15] Zhao J, Zhang L, Wang S. Measurement and evolution law of overburden fracture angle in high cutting stope with composite roof. Coal Engineering. 2021;53(01):75-8.

[16] Zhang J, He Y, Wang X, Feng C. Analysis and Research on Overburden Failure Laws Under Repeated Mining in Shallow-buried and Close Coal Seam Group. Ming Research & Development. 2022;42(02):60-4.

[17] Z. P, D. CL. Modelling permeability for coal reservoirs: A review of analytical models and testing data - ScienceDirect. International Journal of Coal Geology. 2012;92(01):1-44.

[18] Wang X, Li X, Xu D. Migration Rule of Coal Seam Floor in Gob Area and Numerical Simulation of Seepage-stress Coupling. Coal Technology. 2016;35(07):30-2.

[19] Zhang C, Tu S, Zhang L. Analysis of broken coal permeability evolution under cyclic loading and unloading conditions by the model based on the hertz contact deformation principle. Transport in Porous Media. 2017;119(03):739-54.

[20] Wang D, Wang J, Wei J, Wei L. A fluid solid coupling model of coal seam gas considering gas multi-mechanism flow and a numerical simulation analysis of gas drainage. Journal of China Coal Society. 2023;48(02):763-75.

[21] Liu G, Zhang W, Zou Y, Chai H, Xue Y. Numerical Study on Characteristics of Bedrock and Surface Failure in Mining of Shallow-Buried MCS. Energies. 2022;15(9):3446.

[22] Xue J, Zhao T. Deformation and Fracture Characteristics of Coal Gangue Interbedded Samples under Loading and Unloading Conditions. Advances in Civil Engineering. 2022;2022.

[23] Gao D, Sang S, Liu S, Wu J, Geng J, Tao W, et al. Experimental study on the deformation behaviour, energy evolution law and failure mechanism of tectonic coal subjected to cyclic loads. International Journal of Mining Science and Technology. 2022;32(6):1301-13.

[24] Ding K, Wang L, Li Z, Guo J, Ren B, S JCa. Comparative Study on the Seepage Characteristics of Gas-Containing Briquette and Raw Coal in Complete Stress-Strain Process. Materials. 2022;15(18):6205.

[25] Tao Y, Du H, Zhang R, Feng J, Deng Z. Experiment Study on Mechanical Evolution Characteristics of Coal and Rock under Three-Dimensional Triaxial Stress. Applied Sciences-Basel. 2022;12(5):2445.

[26] Zhu W, Wei C. Numerical simulation on mining-induced water inrushes related to geologic structures using a damage-based hydromechanical model. Environmental Earth Sciences. 2011;62(01):43-54.

[27] Shi B, Yu Q, Zhou S. Numerical Simulation of Far-Distance Rock Strata Failure and Deformation Caused byMining Protecting Stratum. Journal of China University of Mining & Technology. 2004(03):25-9.

[28] Zhang J, Zhuo Q, Yang S, Yang T, Wang B, Bai W, et al. Study on the Coal Pillar Weakening Technology in Close Distance Multi-Coal Seam Goaf. Energies. 2022;15(18):6532.

[29] He L, Wu D, Ma L. Numerical simulation and verification of goaf morphology evolution and surface subsidence in a mine. Engineering Failure Analysis. 2023;144:106918.

[30] Wei Z, Zhao M, Xie F, Cao S, Dong J, Dong Y. Detection of former goaf and analysis of deformation characteristics of overburden in Dameidong coal mine. Frontiers in Earth Science. 2023;11:1111745.

[31] Tan X, Chen W, Wang L, Qin CK. Spatial deduction of mining-induced stress redistribution using an optimized non-negative matrix factorization model. Journal of Rock Mechanics and Geotechnical Engineering. 2023;15(11):2868-76.

[32] Wu R, Xu J, Kong X, Shi C. Gas Pressure Relief Rule of Overlying Coal Seam Induced by Fully Mechanized Top Coal Caving in Long Working Face. Journal of Mining & Safety Engineering. 2010;27(01):8-12+8.

[33] Wang L, Xu J, Wu R. Theoretical Study on Stress Distinguishing Index of Gas Pressure Fully Released in Mining Seam. Coal Science and Technology. 2012;40(03):1-5.

[34] Li C, Wu S, Zheng C, Sun X, Jiang X. Study on temporal and spatial evolution characteristics of overburden deformation and gas emission during the longwall working face initial mining phase. Journal of Geophysics and Engineering. 2022;19(3):534-49.

[35] Li C, He Y, Sun X, Fu Y. Fracture Evolution Characteristics and Deformation Laws of Overlying Strata during the Initial Period of Longwall Mining: Case Study. Sustainability. 2023;15(11):8596.